

Title	Experimental evidence of Tc enhancement without the influence of spin fluctuations:NMR study on LaFeAsO <sub>1-x</sub> H <sub>x</sub> under a pressure of 3.0 GPa
Author(s)	Kawaguchi, N.; Fujiwara, N.; Iimura, S.; Matsuishi, S.; Hosono, H.
Citation	Physical Review B (2016), 94(16)
Issue Date	2016-10-15
URL	<a href="http://hdl.handle.net/2433/241712">http://hdl.handle.net/2433/241712</a>
Right	© 2016 American Physical Society
Type	Journal Article
Textversion	publisher

## Experimental evidence of $T_c$ enhancement without the influence of spin fluctuations: NMR study on $\text{LaFeAsO}_{1-x}\text{H}_x$ under a pressure of 3.0 GPa

N. Kawaguchi,<sup>1</sup> N. Fujiwara,<sup>1,\*</sup> S. Iimura,<sup>2,3</sup> S. Matsuishi,<sup>2,3</sup> and H. Hosono<sup>2,3</sup>

<sup>1</sup>Graduate School of Human and Environmental Studies, Kyoto University, Yoshida-Nihonmatsu-cyo, Sakyo-ku, Kyoto 606-8501, Japan

<sup>2</sup>Material and Structures Laboratory (MSL), Tokyo Institute of Technology, 4259 Nagatsuda, Midori-ku, Yokohama 226-8503, Japan

<sup>3</sup>Frontier Research Center (FRC), Tokyo Institute of Technology, 4259 Nagatsuda, Midori-ku, Yokohama 226-8503, Japan

(Received 18 February 2016; revised manuscript received 14 September 2016; published 4 October 2016)

The electron-doped high-transition-temperature ( $T_c$ ) iron-based pnictide superconductor  $\text{LaFeAsO}_{1-x}\text{H}_x$  has a unique phase diagram: Superconducting double domes are sandwiched by antiferromagnetic phases at ambient pressure and they turn into a single dome with a maximum  $T_c$  that exceeds 45 K at a pressure of 3.0 GPa. We studied whether spin fluctuations are involved in increasing  $T_c$  under a pressure of 3.0 GPa by using the  $^{75}\text{As}$  nuclear magnetic resonance (NMR) technique. The  $^{75}\text{As}$ -NMR results for the powder samples show that  $T_c$  increases up to 48 K without the influence of spin fluctuations. This fact indicates that spin fluctuations are not involved in raising  $T_c$ , which implies that other factors, such as orbital degrees of freedom, may be important for achieving a high  $T_c$  of almost 50 K.

DOI: [10.1103/PhysRevB.94.161104](https://doi.org/10.1103/PhysRevB.94.161104)

The phase diagram of the electron-doped high-transition-temperature ( $T_c$ ) iron-based pnictide  $\text{LaFeAsO}_{1-x}\text{H}_x$  (H-doped La1111 series) is unique owing to the capability of electron doping: (i) It exhibits a superconducting (SC) phase with double domes covering a wide H-doping range from  $x = 0.05$  to 0.44 [1], (ii) the SC phase is sandwiched by antiferromagnetic (AF) phases appearing in heavily and poorly electron-doped regimes [see Fig. 1(a)] [2], and (iii) the application of pressure transforms the double domes into a single dome [1,3]. Intriguingly, upon applying pressure, the minimum  $T_c$  at ambient pressure becomes the maximum  $T_c$  of over 45 K [1], as shown by the solid arrow in Figs. 1(a) and 4, as described in detail below.

The unique features established in this compound have not been observed so far in other iron-based pnictides, such as the Ba122 and Na111 series, which have been investigated intensively from an early stage because they are available as large crystals. The electronic phase diagram of the Ba122 series is similar to that of high- $T_c$  cuprates [4]. The analogy is reminiscent of the importance of AF fluctuations in iron-based pnictides. The spin-fluctuation-mediated mechanism is a major candidate for the high- $T_c$  mechanism. In fact, the SC phase of the Ba122 series partially overlaps the AF phase, in other words, the SC and AF states are compatible, and the maximum  $T_c$  occurs close to the phase boundary [see Fig. 1(b)] [5,6]. Because of this special location,  $T_c$  is enhanced and low-energy AF fluctuations simultaneously become predominant as the doping level approaches the AF phase [7,8]. The Na111 series has a phase diagram similar to that of the Ba122 series, however, the SC phase overlaps the AF phase over a wide doping range and even extends to the undoped material [9]. By tuning pressure,  $T_c$  and AF fluctuations are found to be related in a similar manner as in the Ba122 series [10]. A pressure-enhanced  $T_c$  occurs in the 11 series FeSe, which is superconducting and has no magnetic orders at ambient pressure. At first sight, the series seems to be free from antiferromagnetism, however, at pressures exceeding 1 GPa,

the SC phase is adjacent to the AF or AF+SC phase [11]. In fact, the influence of AF fluctuations is observable in the SC phase even at ambient pressure [12].

AF fluctuations seem to play a key role in raising  $T_c$  for various iron-based pnictides, however, the scenario does not work well for  $\text{LaFeAsO}_{1-x}\text{F}_x$ , because, for  $x = 0.14$ ,  $T_c$  increases up to 40 K at 3.0 GPa with no predominant AF fluctuations [13,14]. The La1111 series under high pressure is the only material available for investigating the magnetic properties of pnictides with  $T_c$  in the range of 45–50 K. In fact, the Sm1111 series marks the highest  $T_c$  ( $T_c = 55$  K) in all types of iron-based pnictides [15], however, it includes magnetic Sm ions, which hinders the investigation of the magnetic properties of iron-basal planes. The rise of  $T_c$  without AF fluctuations was observed only for  $x = 0.14$  (see the dashed arrow in Fig. 4), because AF fluctuations remain in a lower doping range than  $x = 0.14$  and, unfortunately,  $x = 0.14$  is nearly the highest level of F doping. As far as nuclear magnetic resonance (NMR) studies on  $\text{LaFeAsO}_{1-x}\text{F}_x$  are concerned, the maximum doping level is less than  $x = 0.14$ –0.15 [16,17]. To establish the breakdown of this scenario over a wide doping range ( $0.20 \leq x \leq 0.44$ ) that covers the second SC dome, we applied  $^{75}\text{As}$  ( $I = 3/2$ ) NMR to powder samples of the H-doped La1111 series at 3.0 GPa.

We applied a pressure of 3.0 GPa to samples with  $x = 0.20$ , 0.40, and 0.44. The pressure was applied by using NiCrAl-CuBe hybrid piston-cylinder-type cells. We used a mixture of F-70 and F-77 fluorinate as the pressure mediation liquid. The details of the pressure cells are given in Ref. [18]. A coil wound around the samples inside the pressure cell and capacitors equipped with a NMR probe form the tank circuit, which serves to detect the detuning of the resonance frequency, namely, the ac susceptibility, and to detect the NMR signal as well. The NMR measurements were performed using a conventional coherent pulsed-NMR spectrometer. The  $^{75}\text{As}$ -NMR spectra show a broad powder pattern with double edges [14], which originates from the second-order quadrupole effect under a magnetic field. The relaxation time ( $T_1$ ) for  $^{75}\text{As}$  was measured by using the saturation-recovery method at the lower-field edge in the field-swept NMR spectra. The low-field

\*naoki@fujiwara.h.kyoto-u.ac.jp

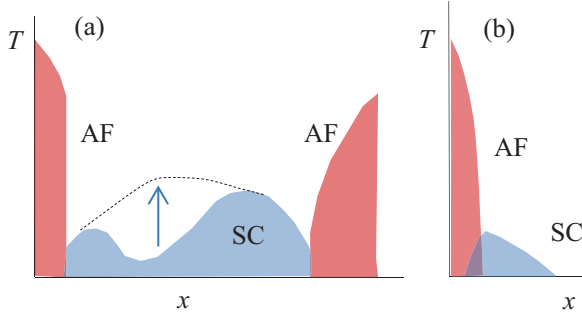


FIG. 1. Schematic phase diagrams of (a) H-doped La1111 series  $\text{LaFeAsO}_{1-x}\text{H}_x$ , and of (b) Ba122 series such as  $\text{Ba}(\text{Fe}_{1-x}\text{Co}_x)_2\text{As}_2$ . AF and SC represent antiferromagnetic and superconducting phases, respectively. The arrow in (a) shows the enhancement of  $T_c$  that occurs between ambient pressure and 3.0 GPa.

edge appears at about 48.2 kOe for an NMR frequency of 35.1 MHz. The signals at the low-field edge come from the powder samples with the iron-basal planes parallel to the applied field. Figures 2(a)–2(c) show the evolution of the relaxation rate ( $1/T_1$ ) divided by temperature ( $T$ ) (i.e.,  $1/T_1T$ ). Here, we chose  $T_c$  as the onset of  $1/T_1T$  just above  $T_c$  (marked as arrows in Figs. 2(a)–2(c)). For  $x = 0.20$ ,  $1/T_1T$  just above  $T_c$  exhibited plateaus, as shown by dotted lines in Fig. 2(a), and  $T_c$  was remarkably enhanced upon applying pressure. For  $x = 0.40$  and 0.44, an anomaly was observed in a paramagnetic state, marked as  $T^*$ , and both  $T^*$  and  $T_c$  were unchanged upon applying pressure. For  $x = 0.44$ , Curie-Weiss-like behavior, which implies AF fluctuations, appears above  $T^*$  at 0.1 MPa, however, this behavior has no appreciable effect on  $T_c$ .

Note that  $T_c$  was determined under the applied field. In general,  $T_c$  decreases more or less under an applied field, however, the decrease is significantly suppressed because we measured  $1/T_1T$  for the powder samples with the iron-basal planes parallel to the applied field. In fact, the values of  $T_c$  are in good agreement with those determined from the detuning of

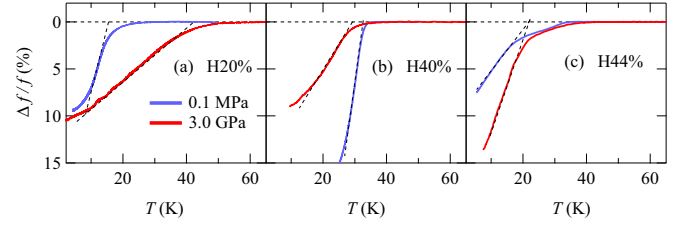


FIG. 3. Detuning of resonance frequency for (a)  $x = 0.20$ , (b)  $x = 0.40$ , and (c)  $x = 0.44$ .  $T_c$ 's determined from  $1/T_1T$  [see arrows in Figs. 1(a)–1(c)] are in good agreement with the extrapolations of dashed lines.

resonance frequency at zero field. In this measurement,  $T_c$  can be determined from the extrapolation, shown as dashed lines in Figs. 3(a)–3(c). Figure 4 shows the doping dependence of  $T_c$  determined from the resistivity [1] and  $1/T_1T$ . The data at 3.0 GPa for the low-doping regime are cited from the results of the F-doped La1111 series [14, 19]. As highlighted by the solid arrow in Fig. 4,  $T_c$  increases to 48 K at 3.0 GPa, which is comparable to the highest  $T_c$  ( $\sim 55$  K) for all types of iron-based superconductors marked in the Sm1111 series.

In general,  $1/T_1T$  of  $d$ -electron systems is determined by spin correlations and is expressed by using the imaginary part of the dynamical spin susceptibility  $\text{Im} \chi(q, \omega)$  as  $1/T_1T \propto \text{Im} \chi(q, \omega_N)/\omega_N$ , where  $\omega_N$  is the angular frequency of nuclei. When the interaction between electrons is significantly strong, namely, spin fluctuations are predominant, Curie-Weiss-like behavior is derived, whereas when the interaction is weak,  $1/T_1T$  is determined by the density of states (DOS) at Fermi surfaces. Unlike other pnictides, Curie-Weiss-like behavior is not observable for  $x = 0.20$ , as seen in Fig. 2(a). Another example is  $\text{K}_y\text{Fe}_{2-x}\text{Se}_2$  with  $T_c = 30$  K [20]: The compound exhibits a similar  $T$  dependence to the La1111 series. The results in Fig. 2(a) demonstrate that  $T_c$  is enhanced without appreciable low-frequency AF fluctuations, which is the most important result for this study. The absence of AF fluctuations

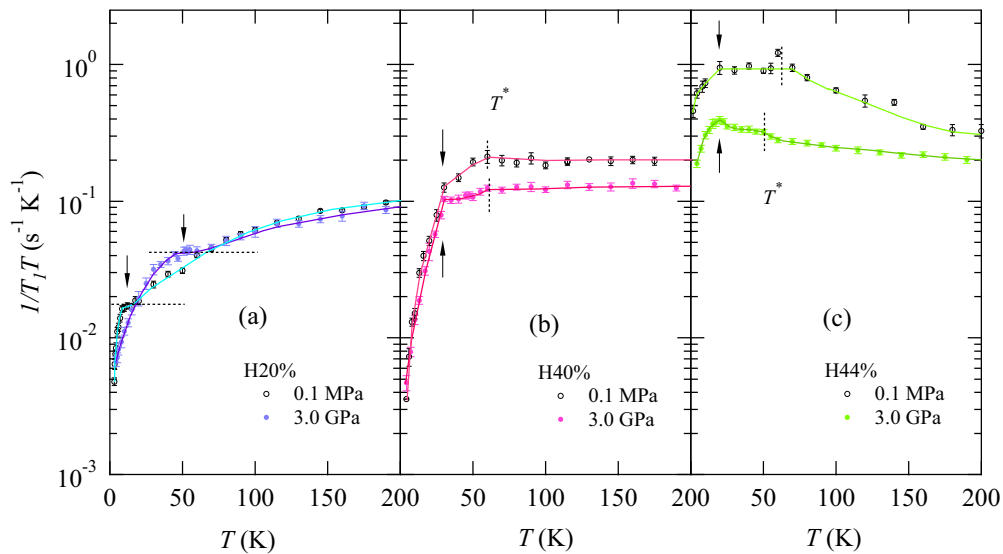


FIG. 2. Nuclear magnetic relaxation rate divided by temperature  $1/T_1T$  for  $^{75}\text{As}$  for (a)  $x = 0.20$ , (b)  $x = 0.40$ , and (c)  $x = 0.44$ . Arrows represent  $T_c$  and solid curves are guides to the eye. Horizontal dotted lines in (a) represent plateaus just above  $T_c$ . For  $x = 0.40$  and 0.44, an anomaly of  $1/T_1T$  appears at  $T^*$  in a paramagnetic phase (see vertical dotted lines).

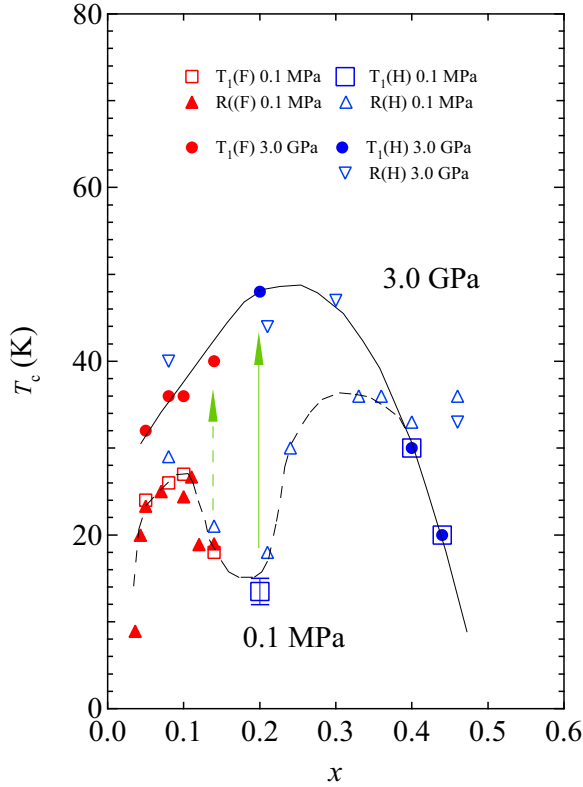


FIG. 4. Phase diagram of  $\text{LaFeAsO}_{1-x}\text{H}_x$  ( $0.05 \leq x \leq 0.5$ ) and  $\text{LaFeAsO}_{1-x}\text{F}_x$  ( $0.05 \leq x \leq 0.14$ ). Solid and open triangles represent  $T_c$  determined by the resistivity at ambient pressure, and open squares represent  $T_c$  determined by the relaxation time ( $T_1$ ). Downward pointing triangles and solid circles represent  $T_c$  determined by the resistivity and  $T_1$  at 3.0 GPa, respectively. The dashed and solid arrows indicate the enhancement of  $T_c$  that occurs when pressure is applied.

has also been confirmed from the neutron scattering measurements in both  $\text{LaFeAsO}_{1-x}\text{H}_x$  [21] and  $\text{LaFeAsO}_{1-x}\text{F}_x$  [22]: An inelastic scattering peak is absent for  $x = 0.20$ , despite the fact that it is unambiguously observable near the AF phase.

Herein, the  $T$  dependence of  $1/T_1T$  is attributable to the DOS. The monotonous  $T$  dependence at high temperatures is attributed to the DOS involved only at high temperatures. In fact, the photoemission spectroscopy measurements demonstrate that the DOS for  $\text{LaFeAsO}_{1-x}\text{F}_x$  decreases with decreasing temperature [23]. This scenario is approved by a quantitative evaluation of  $1/T_1T$  just at the plateau. We evaluate  $1/T_1T$  using the Korringa relation [24,25] for  $d$ -electron alloys [26],

$$1/T_1T = \frac{\pi}{\hbar} (2\hbar\gamma_N A_{\text{hf}})^2 \sum_i n_i(\varepsilon_F)^2 \frac{k_B}{(1 - \alpha_Q)^2}, \quad (1)$$

where  $\gamma_N$ ,  $A_{\text{hf}}$ , and  $n_i(\varepsilon_F)$  represent the gyromagnetic ratio of  $^{75}\text{As}$  (7.292 MHz/10 kOe), the hyperfine coupling constant, and DOS at Fermi surfaces for  $i = d_{xy}$ ,  $d_{yz}$ , and  $d_{zx}$  orbitals, respectively. The factor  $\alpha_Q$  is  $I\chi(Q)$ , where  $I$  is the interaction between electrons and  $\chi(Q)$  is the susceptibility without the interaction at the dominant wave number  $Q$ . The value of  $A_{\text{hf}}$  has been estimated to be  $\sim 25$  kOe/ $\mu_B$  from the  $K$ - $\chi$  plot [27]. The theoretically calculated values of  $n_i(\varepsilon_F)$  for  $x = 0.20$  at

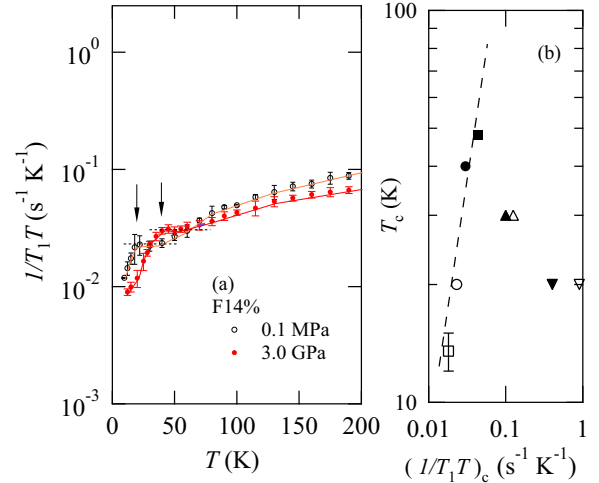


FIG. 5. (a)  $1/T_1T$  for  $\text{LaFeAsO}_{1-x}\text{F}_x$  ( $x = 0.14$ ). Arrows represent  $T_c$ . (b)  $T_c$  vs  $1/T_1T$  at  $T_c$  for  $\text{LaFeAsO}_{1-x}\text{H}_x$  and  $\text{LaFeAsO}_{1-x}\text{F}_x$ . Circles represent the data for  $x = 0.14$  (F doping), and squares, regular triangles, and downward pointing triangles represent those for  $x = 0.20$ ,  $0.40$ , and  $0.44$  (H doping), respectively. Open and solid marks represent the measurements at 0.1 MPa and 3.0 GPa, respectively. The dashed line is a guide to the eye.

ambient pressure are  $0.62$ ,  $0.92$ , and  $0.92$   $\text{eV}^{-1}$ , respectively, for  $i = d_{xy}$ ,  $d_{yz}$ , and  $d_{zx}$  orbitals [1]. These values result in  $1/T_1T = 4.96 \times 10^{-4} \frac{1}{(1 - \alpha_Q)^2}$  ( $\text{s}^{-1} \text{K}^{-1}$ ). The plateau of  $1/T_1T$  at 0.1 MPa indicates  $0.018$   $\text{s}^{-1} \text{K}^{-1}$ , and thus  $\alpha_Q = 0.83$ . The value is in good agreement with the theoretically estimated value  $\alpha_Q = 0.94$  for  $x = 0.20$  [28]. At high temperatures,  $1/T_1T$  at 3.0 GPa is almost the same as that at 0.1 MPa, which suggests that  $\alpha_Q$  is insensitive to pressure and thus  $\alpha_Q$  is not a key parameter for increasing  $T_c$ .

Figure 5(a) shows the plateaus observed for 14% F-doped samples [13,14]. The  $T_c$  enhancement upon applying pressure is highlighted by the dashed arrow in Fig. 4. At 0.1 MPa, the values of  $1/T_1T$  at  $T_c$ ,  $(1/T_1T)_c$ , are  $0.023$  and  $0.018$   $\text{s}^{-1} \text{K}^{-1}$  for 14% F- and 20% H-doped samples, respectively. At 3.0 GPa, these numbers increase to  $0.030$  and  $0.044$ , respectively. These data are plotted in Fig. 5(b). The data for 40% and 44% H-doped samples are also plotted for comparison. As seen from the figure,  $T_c$  correlates with  $(1/T_1T)_c$  only for 14% F- and 20% H-doped samples reflecting  $n_i(\varepsilon_F)$  in Eq. (1).

Our results for the La1111 series demonstrate that  $T_c$  is not directly affected by AF fluctuations, as clearly seen from Figs. 2(a) and 2(c). Note that the opposite conclusion was derived for the Na111 series, such as  $\text{NaFe}_{1-x}\text{Co}_x\text{As}$  [10]. In the Na111 series,  $T_c$  follows AF fluctuations when pressure is applied. At first glance, the results of the Na111 series seem to contradict the results reported herein. One may classify the La1111 series as an exotic and exceptional compound among iron-based pnictides. However, all facts including the La1111 and Na111 series are consistent if the superconductivity is not directly affected by antiferromagnetism or AF fluctuations. For all iron-based pnictides, without exception,  $1/T_1T$  becomes stronger as the doping level approaches the AF phase boundary, but the  $T_c$  optimal doping level is not always located on the AF phase boundary and depends on the compounds, which causes an apparent discrepancy.

Roughly speaking,  $T_c$  is proportional to the DOS and the pairing interaction. The enhancement of the pairing interaction is hardly expected for the AF-fluctuation-mediated scenario. As another candidate, the orbital-fluctuation-mediated scenario [28] would be promising. In this case, orbital fluctuations are difficult to observe in  $1/T_1T$  at a doping level where the structural or nematic phase is absent, and thus the increase in  $T_c$  is observable via the DOS alone in  $1/T_1T$ . To investigate whether the pairing interaction is enhanced simultaneously as well as the DOS, further theoretical investigations are needed, however, the results of Fig. 5(b) may give an important clue.

One may consider another scenario where the pairing interaction originates from AF fluctuations, but AF fluctuations are suppressed at ambient pressure by some competing interactions, such as orbital and/or charge interactions. On the basis of this scenario,  $T_c$  could be suppressed and the double-dome structure could be observed, as seen in some high- $T_c$  cuprates. Pressure could nullify the competition, and  $T_c$  may increase under pressure even if AF fluctuations are

not enhanced. However, the competing orders, which could cause an appreciable suppression of  $T_c$ , have not been observed so far in a wide range around  $x = 0.14$ – $0.20$ . Furthermore, AF fluctuations tend to decrease upon applying pressure, as observed in the poorly F-doped regime [29] or sufficiently H-doped regime [see Fig. 1(c)]. At present, there is no experimental evidence to support this scenario.

In conclusion, we have observed in  $\text{LaFeAsO}_{1-x}\text{H}_x$  that  $T_c$  for  $x = 0.20$  marks a high  $T_c$  of 48 K upon applying pressure without the influence of AF fluctuations. For  $x = 0.44$  (near the second AF phase boundary),  $T_c$  remains unchanged without depending on the magnitude of AF fluctuations. These results suggest that the superconductivity has no direct connection with AF fluctuations. As far as the results of  $1/T_1T$  are concerned, the increase in  $T_c$  up to 48 K originates from an enhancement of the DOS just above  $T_c$ .

The authors thank H. Kontani and Y. Yamakawa for discussions.

- 
- [1] S. Iimura, S. Matsuishi, H. Sato, T. Hanna, Y. Muraba, S. W. Kim, J. E. Kim, M. Takata, and H. Hosono, *Nat. Commun.* **3**, 943 (2012).
- [2] N. Fujiwara, S. Tsutsumi, S. Iimura, S. Matsuishi, H. Hosono, Y. Yamakawa, and H. Kontani, *Phys. Rev. Lett.* **111**, 097002 (2013).
- [3] H. Takahashi, H. Soeda, M. Nukii, C. Kawashima, T. Nakanishi, S. Iimura, Y. Muraba, S. Matsuishi, and H. Hosono, *Sci. Rep.* **5**, 7829 (2014).
- [4] I. I. Mazin, *Nature (London)* **464**, 183 (2010).
- [5] S. Nandi, M. G. Kim, A. Kreyssig, R. M. Fernandes, D. K. Pratt, A. Thaler, N. Ni, S. L. Bud'ko, P. C. Canfield, J. Schmalian, R. J. McQueeney, and A. I. Goldman, *Phys. Rev. Lett.* **104**, 057006 (2010).
- [6] H. Chen, Y. Ren, Y. Qiu, W. Bao, R. H. Liu, G. Wu, T. Wu, Y. L. Xie, X. F. Wang, and Q. Huang, *Europhys. Lett.* **85**, 17006 (2009).
- [7] F. L. Ning, K. Ahilan, T. Imai, A. S. Sefat, M. A. McGuire, B. C. Sales, D. Mandrus, P. Cheng, B. Shen, and H.-H. Wen, *Phys. Rev. Lett.* **104**, 037001 (2010).
- [8] Y. Nakai, T. Iye, S. Kitagawa, K. Ishida, H. Ikeda, S. Kasahara, H. Shishido, T. Shibauchi, Y. Matsuda, and T. Terashima, *Phys. Rev. Lett.* **105**, 107003 (2010).
- [9] A. F. Wang, X. G. Luo, Y. J. Yan, J. J. Ying, Z. J. Xiang, G. J. Ye, P. Cheng, Z. Y. Li, W. J. Hu, and X. H. Chen, *Phys. Rev. B* **85**, 224521 (2012).
- [10] G. F. Ji, J. S. Zhang, L. Ma, P. Fan, P. S. Wang, J. Dai, G. T. Tan, Y. Song, C. L. Zhang, P. Dai, B. Normand, and W. Yu, *Phys. Rev. Lett.* **111**, 107004 (2013).
- [11] M. Bendele, A. Ichsanow, Yu. Pashkevich, L. Keller, Th. Strässle, A. Gusev, E. Pomjakushina, K. Conder, R. Khasanov, and H. Keller, *Phys. Rev. B* **85**, 064517 (2012).
- [12] S.-H. Baek, D. V. Efremov, J. M. Ok, J. S. Kim, J. van den Brink, and B. Büchner, *Nat. Mater.* **14**, 210 (2015).
- [13] K. Tatsumi, N. Fujiwara, H. Okada, H. Takahashi, Y. Kamihara, M. Hirano, and H. Hosono, *J. Phys. Soc. Jpn.* **78**, 023709 (2009).
- [14] T. Nakano, N. Fujiwara, K. Tatsumi, H. Okada, H. Takahashi, Y. Kamihara, M. Hirano, and H. Hosono, *Phys. Rev. B* **81**, 100510(R) (2010).
- [15] Z.-A. Ren, W. Lu, J. Yang, W. Yi, X.-L. Shen, Z.-C. Li, G.-C. Che, X.-L. Dong, L.-L. Sun, F. Zhou, and Z.-X. Zhao, *Chin. Phys. Lett.* **25**, 2215 (2008).
- [16] F. Hammerath, U. Gräfe, T. Kühne, P. L. Kühne, A. P. Reyes, G. Lang, S. Wurmehl, B. Büchner, P. Carretta, H.-J. Gräfe, *Phys. Rev. B* **88**, 104503 (2013).
- [17] T. Oka, Z. Li, S. Kawasaki, G. F. Chen, N. L. Wang, and G.-q. Zheng, *Phys. Rev. Lett.* **108**, 047001 (2012).
- [18] N. Fujiwara, T. Matsumoto, K. Koyama-Nakazawa, A. Hisada, and Y. Uwatoko, *Rev. Sci. Instrum.* **78**, 073905 (2007).
- [19] T. Nakano, N. Fujiwara, Y. Kamihara, M. Hirano, H. Hosono, H. Okada, and H. Takahashi, *Phys. Rev. B* **82**, 172502 (2010).
- [20] W. Yu, L. Ma, J. B. He, D. M. Wang, T.-L. Xia, G. F. Chen, and W. Bao, *Phys. Rev. Lett.* **106**, 197001 (2011).
- [21] S. Iimura, S. Matsuishi, M. Miyakawa, T. Taniguchi, K. Suzuki, H. Usui, K. Kuroki, R. Kajimoto, M. Nakamura, Y. Inamura, K. Ikeuchi, S. Ji, and H. Hosono, *Phys. Rev. B* **88**, 060501(R) (2013).
- [22] S. Wakimoto, K. Kodama, M. Ishikado, M. Matsuda, R. Kajimoto, M. Arai, K. Kakurai, F. Esaka, A. Iyo, H. Kito, H. Eisaki, and S. Shyamoto, *J. Phys. Soc. Jpn.* **79**, 074715 (2010).
- [23] T. Sato, K. Nakayama, Y. Sekiba, T. Arakane, K. Terahima, S. Souma, T. Takahashi, Y. Kamihara, M. Hirano, and H. Hosono, *J. Phys. Soc. Jpn.* **77**, 65 (2008).
- [24] A. Narath and H. T. Weaver, *Phys. Rev.* **175**, 373 (1968).
- [25] T. Moriya, *J. Phys. Soc. Jpn.* **18**, 516 (1963).
- [26] T. Asada and K. Terakura, *J. Phys. F* **12**, 1387 (1982).
- [27] H.-J. Gräfe, G. Lang, F. Hammerath, D. Paar, K. Manthey, K. Koch, H. Rosner, N. J. Curro, G. Behr, J. Werner, N. Leps, R. Klingeler, H.-H. Klauss, F. J. Litterst, and B. Büchner, *New J. Phys.* **11**, 035002 (2009).
- [28] S. Onari, Y. Yamakawa, and H. Kontani, *Phys. Rev. Lett.* **112**, 187001 (2014).
- [29] N. Fujiwara, T. Nakano, Y. Kamihara, and H. Hosono, *Phys. Rev. B* **85**, 094501 (2012).